Modeling the PAAc-AN-TV Surface Using ^{134}Cs and $^{152+154}Eu$ Sorption

Bela El-Gammal, Gehan M. Ibrahim, Karam F. Allan, Ibrahim M. El-Naggar

Hot Laboratories Centre, Atomic Energy Authority, Cairo, Egypt

Received 1 February 2008; accepted 11 February 2009
DOI 10.1002/app.30248
Published online 8 May 2009 in Wiley InterScience (www.interscience.wiley.com).

ABSTRACT: A novel composite, composed of poly (acrylic acid (AAc), acrylonitrile, and titanium vanadate, was prepared by induced gamma irradiation route at 20 kGy to be used as a hybrid organic-inorganic sorbent. 5–200 μm particle diameters of the composite were obtained. An average particle size of 75 μm of crystalline (17-20) composite was used; it was thermally stable to 486°C. The distribution coefficients of Cs^+ and Eu^{3+} were studied as a function of pH; 2350 $mL.g^{-1}$ and 645 $mL.g^{-1}$ were obtained in case of $^{152+154}Eu$ and ^{134}Cs at pH 6. 1.55 $mmol.g^{-1}$ and 1.85 $mmol.g^{-1}$ maximum loadings were accommodated for the same ions at the same pH. Different models were used to scan the surface of the exchanger, so that the topography of the surface was studied as a function of surface active site types, concentrations, and heterogeneity. Langmuir, Freundlich and D-R models were used. Also, different kinetic models, as Lagergren pseudo first-order, pseudo second-order and Morris-Weber intraparticle diffusion models were applied to study the possible mechanism of the sorption process; pseudo first-order was exempted to investigate the mechanism. They proved that chemisorption and ion exchange mechanism with controlled diffusion are predominant, with their characteristic mean energies (8.731 $kJ.mol^{-1}$ and 9.310 $kJ.mol^{-1}$ for Cs^+ and Eu^{3+}, respectively). Double Shell Model was finally adopted to explain the suggested mechanism. Negative values of $\Delta G°$, −2.15 $kJ.mol^{-1}$ to −7.92 $kJ.mol^{-1}$ in case of Cs^+ and −3.35 $kJ.mol^{-1}$ to −9.67 $kJ.mol^{-1}$ in case of Eu^{3+}adsorption at different temperatures, indicate the spontaneous nature of the reactions. © 2009 Wiley Periodicals, Inc. J Appl Polym Sci 113: 3405–3416, 2009

Key words: composites; PAAc-AN-TV; kinetics; Isotherms; double shell model and thermodynamics

INTRODUCTION

Waste effluents arisen from nuclear facilities like mining and milling of uranium ores, fuel fabrication, and operation in nuclear power plants cause pollution which is one of the major environmental problems that has to be controlled or solved.[1] Since their undesired effects on human physiology and ecological systems, radionuclides should be removed from the waste streams before their discharge.[2]

Well known radioactive nuclides removal techniques from nuclear waste effluents are settled which include chemical precipitation, membrane filtration, ion exchange, sorption, and coprecipitation. These methods rarely provide satisfactory removal rate to meet the pollution control limits; also, they are expensive in many cases.[3] Therefore low-cost alternative technologies or sorbents are needed for radioactive wastewater treatment.[4]

The selection of a certain sorbent or a common resin is based on the concept of hard and soft acids and bases, i. e., soft cations are removed via adsorption by soft basic groups and vice versa.[5–7]

During the last several decades, researchers have been trying to produce new polymeric materials with specific properties for specific applications. These materials include polymer blends, polymer composites etc.[8]

Some inorganic–organic polymer composites have recently been the subject of intense interest because of their electrical, optical, catalytic and mechanical properties.[9]

Due to high adsorption selectivity, irradiation resistance, thermal and chemical stabilities, composites have found wide use in treatment of aqueous nuclear waste.[9–12] The treatment options based on adsorption and ion exchange phenomena play an important role in pre-concentration and separation of toxic radionuclides from aqueous wastes. In these patterns, the texture of the composite surface was insufficiently described.[13–15]

Therefore, this work is intended to prepare novel composite materials, based on vinyl polymers and titanium vanadate ion exchanger with extensive description of the composite surface using different models; new approach were tried to scan the surface of the composites and compared with other models.

Correspondence to: B. El-Gammal (belalelgammal@hotmail.com).

EXPERIMENTAL

All reagents were of analytical grade and used without further purification. Acrylic acid and acrylonitrile monomers were purchased from Merck Chemical Company, Germany. Titanium tetrachloride and vanadium pentoxide were supplied by Sigma-Aldrich Company, USA.

Radioactive tracers ^{134}Cs (half life = 2.056 year) and $^{152+154}$Eu (half life = 13.4 year) artificially produced in Egyptian Nuclear Reactor, ERR-2, Inshas Site, were finally used in the form of the corresponding nitrates.

Preparation of the exchanger

A solution of 1*M* titanium (IV) chloride was gradually added to 1*M* solution of vanadium chloride (obtained by dissolution of vanadium pentoxide in 0.1*M* HCl followed by evaporation and redissolution in bidistilled H_2O). The reaction was carried out in 2 : 1 volumetric ratio with constant stirring at room temperature. After the addition was completed, ammonia solution was added until complete precipitation of the titanium vanadate. The solution mixture was allowed for settling along a period of 24 h. The precipitate was filtered, washed several times with bidistilled water until the pH of the supernatant reached a constant value at 6.8. The precipitate was filtered again with the aid of centrifugation (10^4 rpm), dried at 50°C in an electric oven, ground and sieved for different mesh sizes and stored at room temperature.

The obtained titanium vanadate was impregnated with a mixture of 60 : 40 wt % (AAc-AN) comonomers in deoxygenated water. The mixture was subjected to 20 kGy gamma irradiation dose from a ^{60}Co unit at a dose rate of 10 kGy/h. After complete polymerization, the obtained composite was dried at 50°C overnight to a constant weight and then ground to the desired mesh size (5-200 μm) and stored for further experimental use.

Characterization

The crystalline content of the end-product was assayed by X-ray diffraction (XRD) using a Shimadzu X-ray diffractometer, Model XD 490(Japan) with nickel filter and Cu-k_α radiation.

IR spectrum of the prepared composite was performed from 400–4000 cm^{-1} using BOMEM FTIR Model 157, Canada.

Thermal analysis, simultaneous DTA-TGA was used as a complementary technique to study the thermal stability of the prepared composite. A separate Shimadzu DTA and TGA thermal analysis stations, Shimadzu-TA50 series, Shimadzu, Japan, were used. Combination of the DTA-TGA was achieved using Shimadzu software.

N_2 adsorption isotherms at 77 K were recorded on an automatic Nova 3000 series built setup, Quantachrome, USA. High vacuum, lower than 10^{-4} Pa, was ensured by a turbo-molecular pump. Pressures were measured by using a 0–1000 Pa and a 0–100,000 Pa Baratron type pressure sensors provided by Edwards, England. N_2 saturation pressure was recorded in situ by using an independent pressure sensor of the same type. Before adsorption, samples were outgassed overnight at 120°C and under a residual pressure of 0.01Pa. Nitrogen (purity>99.9995%) used for experiments was provided by IAG Gas Corporation, Egypt. Specific surface areas (SSAs) were determined by applying the Brunauer–Emmet–Teller (BET) equation[16] and by using 16.3A°^{2} for a cross-sectional area of nitrogen.[17] In the present study, the error of determination of the SSA was ±1 $m^2.g^{-1}$. Micropores volumes and open surface areas were obtained from the t-plot method.[18] As some samples appear microporous, surface areas derived from micropores volumes and open surface areas are more accurate than BET surface area. Thus, total surface areas given were derived from the t-plot analysis.

Batch distribution studies

The uptake of ^{134}Cs and $^{152+154}$Eu individually on PAAc-AN-TV was studied by shaking 4 mL of the aqueous solution containing $10^{-4}M$ of the studied nuclide with 0.02 g of the composite in a shaker water bath for the desired time at 25°C ± 1°C. Thereafter, 2 mL of the shaken solution was withdrawn for radiometric assay using NaI-Tl Scintillation detector connected to Nucleus Counting System, Enterprise, USA. The percentage uptake, *U*% on the solid could be calculated as:

$$U\% = \frac{C_o - C}{C_o} * 100 \quad (1)$$

where C_o is the initial concentration of the metal ion, C is the equilibrium concentration; C_o and C are measured in terms their initial and final radionuclide activities and the standard deviation for counting were taken into consideration. The distribution coefficient, k_d ($mL.g^{-1}$), could be also calculated as

$$k_d = \frac{C_o - C}{C} * \frac{V}{m} \quad (2)$$

where V is the solution volume and m is the weight of the solid composite absorber.

Kinetic experiments

Rate of adsorption for a specific cation was followed up by using Penicillin bottle containing 10 mL of aqueous solutions of ^{134}Cs and $^{152+154}$Eu $10^{-4}M$ in

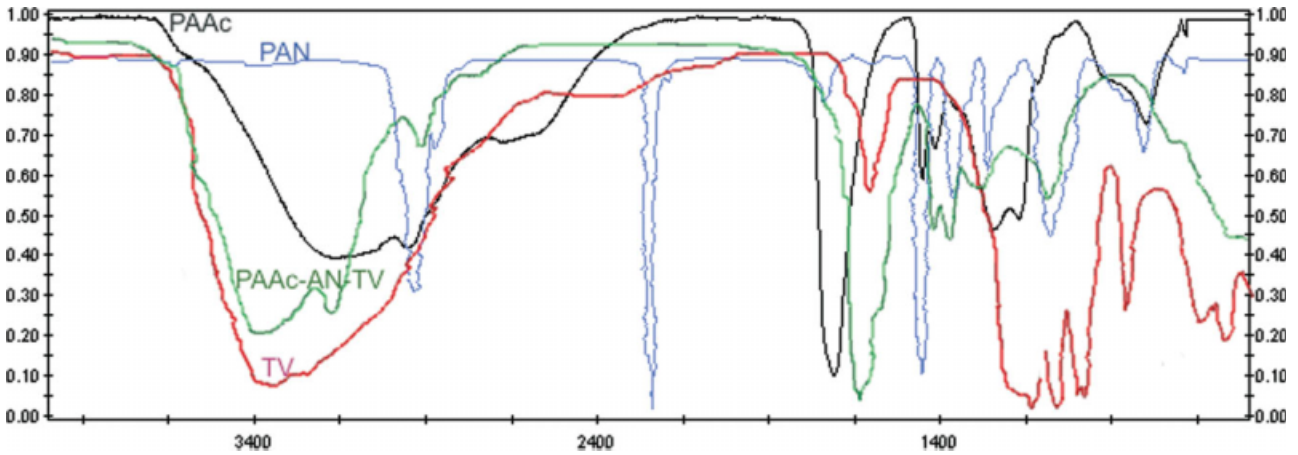

Figure 1 FTIR spectra of PAAc, PAN, TV and the composite PAAc-AN-TV. [Color figure can be viewed in the online issue, which is available at www.interscience.wiley.com]

which 0.05 g from prepared PAAc-AN-TV composite was added; 75 μm particle size was used. The bottles were kept in a thermostated shaker bath at 25°C ± 1°C for various periods of time. Adsorption of nuclides on PAAc-AN-TV was followed with time in stepwise 30 min. and continued till 24 h for different batches.

Adsorption isotherms

Once the equilibrium time was known, the adsorption isotherms could be determined for each nuclide. For this purpose, 10 mL of aqueous solutions of 10^{-6}–10^{-2}M of ^{134}Cs and $^{152+154}$Eu was shaken at 100 rpm with 0.05 g of PAAc-AN-TV, for 24 h at 25°C ± 1°C. After the predetermined sorption time, solution was filtered and the metal ion concentrations were measured. Initial and equilibrium metal ion concentrations in the aqueous solutions were determined radiometrically.

Initial pH of the solutions was adjusted by adding hydrochloric acid or liquid ammonia solutions to the medium to maintain a constant pH. A HANA 30X model pH meter was used to adjust a desired pH value. The pH of the solution was buffered only at 4, except for as stated elsewhere.

Since sorption experiments were temperature controlled, temperature influence experiments were carried out between 25°C and 60°C ± 1°C at optimum pH values for each metal ion. Experiments were repeated three times in each case. The amount of sorbed metal ion was calculated from the change in the metal concentration in the aqueous solution before and after equilibrium and the weight of the dry composite; the amount of metal ion adsorbed by PAAc-AN-TV was calculated as:

$$q = \frac{(C_o - C)}{W} * V \qquad (3)$$

where q is the amount of metal ions adsorbed onto unit amount of the resin (mmol.g^{-1}). C_o and C are the concentrations of metal ions in the initial and equilibrium concentrations of the metal ions in aqueous phase (mmol.L^{-1}), V is the volume of the aqueous phase (L) and W is the dry weight of the resin (g).

RESULTS AND DISCUSSION

Characterization of materials

PAAc-AN-TV has been characterized using FTIR, XRD, DTA-TGA and surface area measurements.

The FTIR spectra of PAAc, PAN, TV and the composite PAAc-AN-TV are shown in Figure 1. Two bands corresponding to –OH carboxylic group at about 3200-3500 cm^{-1} were recorded. The characteristic carbonyl group was found in the 1700 cm^{-1} region. A weak and slightly broad band at about 2700 cm^{-1} was observed, which is due to the single -C—H group as saturated hydrocarbon in the polyacrylic acid; This peak was sharp in case of poly acrylonitrile at about the same region. Also, at 2200-2350 cm^{-1}, a sharp peak was observed, which may be attributed to the –CN group in the triple bond region of polyacrylonitrile. This band may undergo red shift o lower frequency by substitution of the beta-carbon atom. In case of titanium vanadate, multipeaks were observed in the low frequency region, which may be attributed to the V(IV)-O (600 cm^{-1}), -V=O (1035 cm^{-1}), -O—V (1003 cm^{-1} in the g-state), -Ti=O (1087 cm^{-1}), Ti(IV)-O (625 cm^{-1}), and -O-Ti (1005 cm^{-1} in the g-state). In formation of the composite material, the carbonyl and nitrile peaks are shifted and destroyed as seen in figure, which may be assigned to their consumption in the reaction with titanium vanadate to form the resin with the

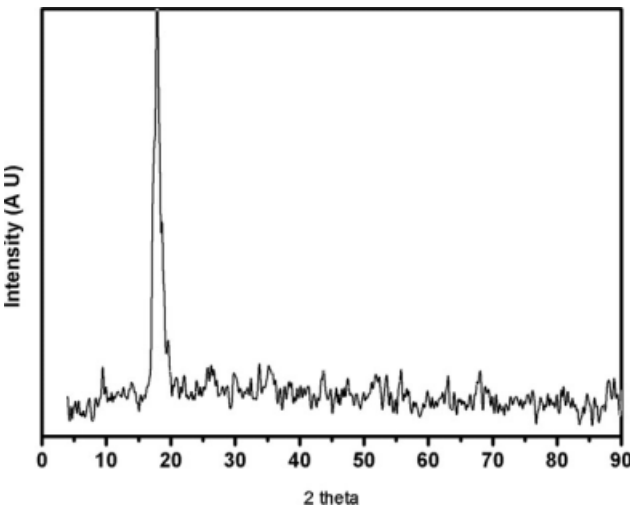

Figure 2 XRD spectrum of PAAc-AN-TV.

formation of partial single -C—O bond in the 1300 cm^{-1} region.[19]

The X-ray diffraction patterns of the different materials were studied. Polyacrylic acid and titanium vanadate were found to be of amorphous structures.[20–25] However, polyacrylonitrile shows only one peak at about 17-20. This peak remains unchanged on formation of the composite material as shown in Figure 2. The degree of crystallinity obtained were in a good a agreement with those obtained when PAN is involved in formation of inorganic and organic composite membranes with yttrium stabilized with ziroconia, as well as PAN nanocomposites.[26–29]

Thermal analysis brief description of simultaneous DTA-TGA of the examined PAAc-AN-TV, indicated that two endotherms were observed at about 86°C and 314°C. They were accompanied by distinct losses in weight as 4.1 wt % and 3.6 wt % at the same temperatures, which may be explained by the removal of free and interstitial waters, respectively. The third weight loss step was observed at about 486°C–720°C, due to decomposition of the polymeric resins and formation of inorganic oxide phase, as recorded by an exothermic peak,[24] is an advantage over the use of PAAc-AN copolymeriztion. Also, radiation stability due composite formation may be greatly enhanced.[27]

Effect of pH

Sorption phenomenon of metal ions by resins is pH dependent; this may be assigned to the discrepancies in either their possible complexation reactions or physisorption processes at the adsorption surface. Since PAAc-AN-TV has various functional groups on its natural structure,[1] effect of pH on sorption capacities should be investigated. The effect of pH

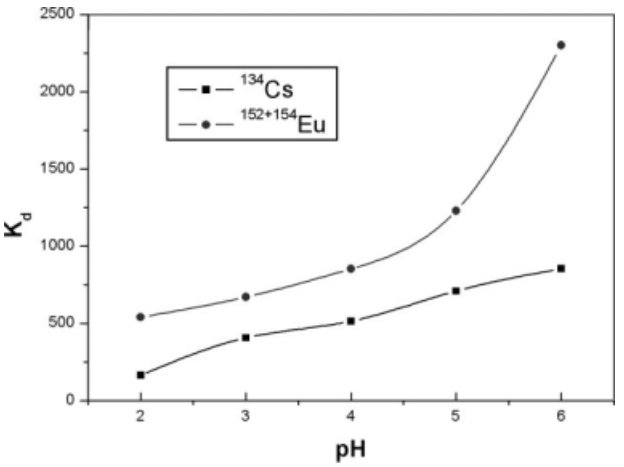

Figure 3 Effect of pH on distribution coefficients of ^{134}Cs and $^{152+154}$Eu sorbed onto PAAc-AN-TV.

on the specific sorption of metal ions by PAAc-AN-TV has shown in Figures 3, 4. k_d increased with increasing pH up to an optimum pH of 6; 2350 $mL.g^{-1}$ and 645 $mL.g^{-1}$ were obtained in case of $^{152+154}$Eu and ^{134}Cs, respectively. The resin exhibited low affinity towards ^{134}Cs and $^{152+154}$Eu at pH 4 or lower that can be attributed to the competitive sorption of H_3O^+ ions and metal ions for the same active sorption sites. This behavior may be further explained with the functional groups introduced to the PAAc-AN-TV. These functional groups must have taken part in metal uptake process by complexation which is pH dependent, and the nature of the active sites and sorbate must have been changed with pH.[3,30] After the optimized pH, sorption capacity (1.55 $mmol.g^{-1}$ and 1.85 $mmol.g^{-1}$ for ^{134}Cs and $^{152+154}$Eu, respectively) started to decrease with increasing the pH of 6; non-linear behavior in case of trivalent europium was observed.

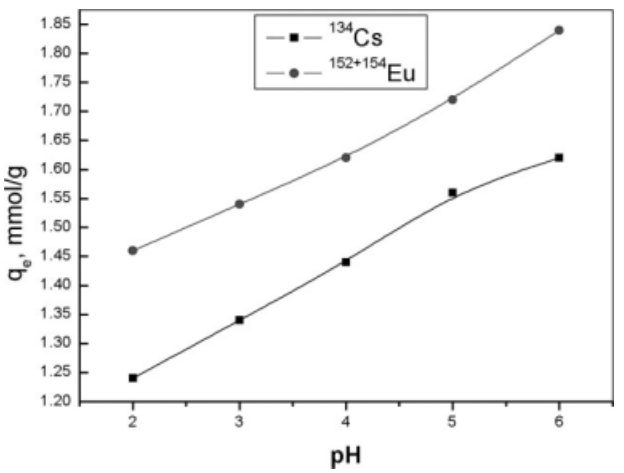

Figure 4 Effect of pH on q_c of ^{134}Cs and $^{152+154}$Eu sorbed onto PAAc-AN-TV.

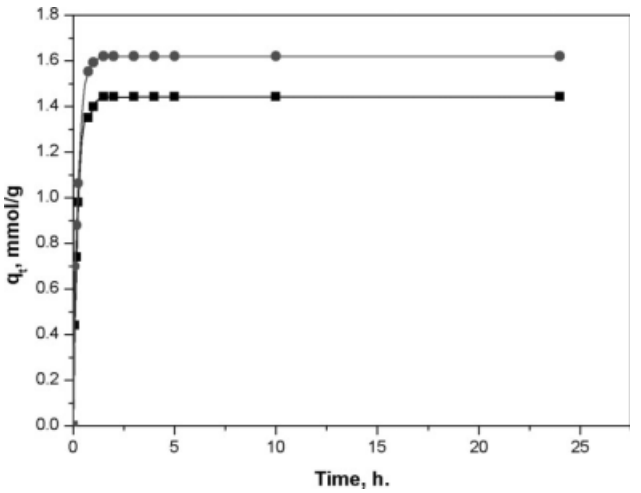

Figure 5 Effect of time on q_t of ^{134}Cs and $^{152+154}$Eu sorbed onto PAAc-AN-TV.

Effect of contact time and sorption dynamics

The influence of contact time on ^{134}Cs and $^{152+154}$Eu uptake capacities has been shown in Figure 5. Rapid uptake kinetics and sorption equilibrium would be accepted to be attained within the first 25 min.; otherwise stated, 1 h of equilibration time was chosen as the optimum contact time to ensure that equilibrium conditions were achieved. In kinetic considerations, the presence of functional groups on a composite should be taken into account. The composite surface should be evaluated according to the accessibility of the ion to the active groups without steric hindrance, which is greatly dependent on the shape and type of polymeric matrices.[1,31]

The key parameters of the sorption rates, like structural properties of the sorbent, metal ion properties, initial concentration of metal ions, pH, temperature, complex formation rate or presence of competing ions were taken into account.

Different kinds of mechanisms as mass transfer, diffusion control, chemical reaction, and particle diffusion may control the kinetics. In this work, the kinetics is primarily subjected to different rate kinetic empirical formulae, including pseudo first-order, pseudo second-order, and intraparticle models.

First-order kinetics

First-order kinetics is expressed as the solute removal rate that controls the residence time of the sorbate in the solid-solution interface. Lagergren and Svenska[32] derived the pseudo first-order rate expression based on solid capacity, q, which is generally expressed as follows:

$$\frac{dq}{dt} = k_{\text{ads}}(q_e - q) \tag{4}$$

Integration of eq. (4) with the boundary conditions as follows: at $t = 0$, $q = 0$, and at $t = t$, $q = q_t$, gives

$$\log(q_e - q_t) = \log q_e - \left(\frac{k_{\text{ads}}}{2.303}\right) t \tag{5}$$

Equation (5) can be written in its non-linear form as

$$q_t = q_e(1 - \exp(-k_{\text{ads}}t)) \tag{6}$$

where q_e and q_t are the amounts of the metal ions adsorbed (mmol.g^{-1}) at equilibrium and at time t (h), respectively, and k_{ads} is the sorption rate constant (time^{-1}). Hypothetically, to ascertain the rate constants and equilibrium metal ion uptake, the straight line plots of $\log(q_e\text{-}q_t)$ against t of eq. (5) should be constructed; the rate constants (k_{ads}) and theoretical equilibrium sorption capacities, q_e (theo.), can be calculated from the slopes and intercepts. In Figure 6 Lagergren's plots and constants related to these plots are given in Table I.

Fitness of straight lines obtained from Lagergren's plots is not a clear parameter to accept the model; it is also required that theoretically calculated equilibrium sorption capacities, q_e (theo.), should be in accordance with the experimental sorption capacity, q_e (exp.), values. As can be seen from Table I, linear correlation coefficients of the plots, for ^{134}Cs and $^{152+154}$Eu are variant. Also, great discrepancies between q_e (theo.) and q_e (exp.), $\pm$0.1 to 0.7 mmol.g^{-1} differences were observed. So, it could be suggested that the adsorption of ^{134}Cs and $^{152+154}$Eu ions onto PAAc-AN-TV is not a first-order reaction. This fact was encountered in numerous systems[33–37] in a comparison with other systems, the first-order parameters for Cs^+ sorbed onto pre-treated arca shell were found to be 0.0386 mmol.g^{-1} and 0.017 min^{-1}, and 0.07899

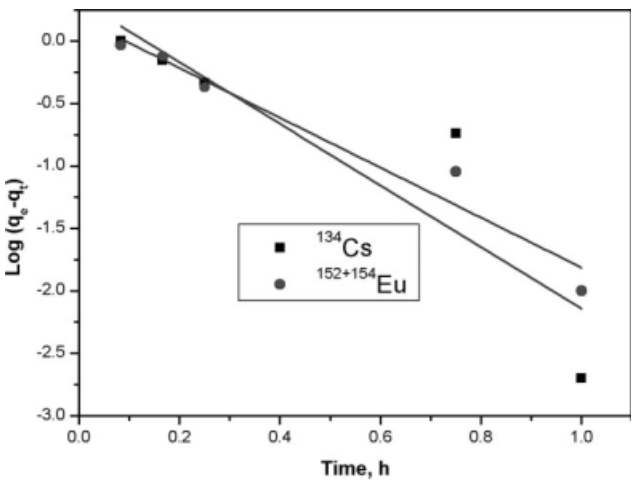

Figure 6 Effect of time on $\log(q_e\text{-}q_t)$ of ^{134}Cs and $^{152+154}$Eu sorbed onto PAAc-AN-TV.

TABLE I
First-Order, Second-Order, and Intraparticle Diffusion Rate Model Constants

	First-order rate constants				Second-order rate constants			Intraparticle diffusion constants	
Ion	q_e(exp.) (mmol.g^{-1})	k_{ads} (h^{-1})	q_e(theo.) (mmol.g^{-1})	R^2	k_2 (mmol.g^{-1}.h^{-1})	q_e(theo.) (mmol.g^{-1})	R^2	k_{id} (mmol.g^{-1}.h$^{-1/2}$)	R^2
Cs^+	1.442	5.679451	2.110564	0.74133	10.16514	1.448604	0.99989	1.4122	0.94977
Eu^{3+}	1.62	4.602522	1.533216	0.94444	13.83784	1.624907	0.99995	1.57737	0.92307

mmol.g^{-1} and 0.58 min.$^{-1}$ for Cr^{3+} sorbed onto a composite material.[38,39]

Second-order kinetics

Predicting the rate of adsorption for a given system is among the most important factors in adsorption system design, as the system kinetics determine adsorbate residence time and reactor dimensions.

Pseudo second-order model is derived on the basis of adsorption capacity of the solid phase, expressed as[1]:

$$\frac{d_q}{d_t} = k_2(q_e - q)^2 \tag{7}$$

Integration of eq. (7) with the boundary conditions, at $t = 0$, $q = 0$, and at $t = t$, $q = q_t$, results in

$$\frac{1}{q_e - q_t} = \frac{1}{q_e} + k_2 t \tag{8}$$

Equation (8) can be stated in the linear form as

$$\frac{t}{q_t} = \frac{1}{k_2 q^2{}_e} + \left(\frac{1}{q_e}\right) t \tag{9}$$

where k_2 (mmol.g^{-1} time^{-1}) is the rate constant of pseudo second-order reaction.

Some authors have conducted evaluation of the model using non-linear and linear forms by means of eqs. (8 and 9) using some heavy metals, especially for Cd on a certain biosorbent, to determine the pseudo second-order kinetic parameters.[40] Although, the non linear form could give higher correlation coefficients, the linear form may be used for simplicity, especially when small differences in the correlation coefficients and standard deviations are explicit.

Figure 7 shows the plots obtained from the graphical presentation of the data for the model; the constants related to these plots are given in Table I.

As seen from the results given in Table I, correlation coefficients are much more higher compared to that obtained from the first-order kinetics. Also, theoretical and experimental q_e values are in a good accordance with each other. Therefore, sorption of ^{134}Cs and $^{152+154}$Eu metal ions onto PAAc-AN-TV is thought to follow second-order type reaction kinetics.

The second-order parameters shown in Table I were greater in capacities than di- and trivalent cations sorbent onto some composites[39]; 0.122 mmol.g^{-1} and 1.3 $\times$ 10^{-2} g.mg^{-1}.min^{-1} and 0.0845 mmol.g^{-1} and 18 $\times$ 10^{-2} g.mg^{-1}.min^{-1} for Zn^{2+} and Cr^{3+}, respectively. This may be ascribed to the dual properties of the composite material; ordinary ion exchange processes are rapid and mainly controlled by diffusion, whereas in a composite adsorbent, another step which is slower and controlled either by particle diffusion or by a second-order chemical reaction may be encountered.[6] Furthermore, pseudo second-order kinetics provides best fits to the experimental data for the sorption systems where chemisorption seems significant in the rate controlling step.[41] PAAc-AN-TV behaves as dual adsorbent because of the PAAc-AN-TV functionality present on it and sorption to the resin would take place via valency forces between the metal ions and the sorbent. Therefore, second-order chemical reaction kinetics would be expected to be followed in the sorption.

Intraparticle diffusion

The Weber and Morris, WM sorption kinetic model was initially employed to describe the removal of some biologically resistant pollutants from waste waters by sorption.[42] as:

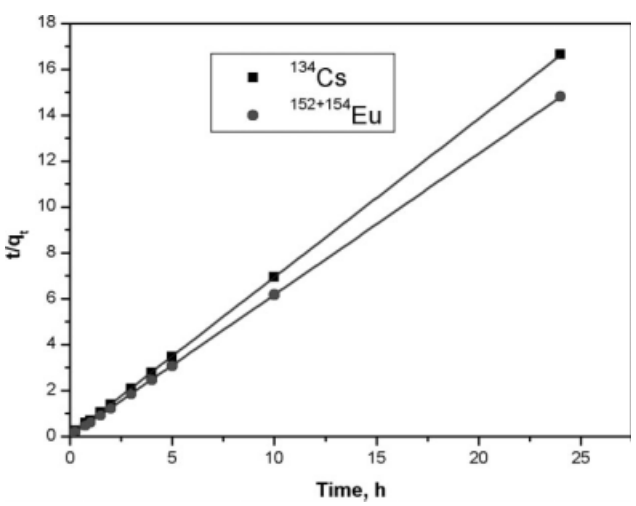

Figure 7 Effect of time on t/q_t of ^{134}Cs and $^{152+154}$Eu sorbed onto PAAc-AN-TV.

$$q_t = k_{id} t^{1/2} \quad (10)$$

In this model investigation, two main mechanisms were used to regulate the model, i.e., intraparticle diffusion and external mass transfer. The intraparticle diffusion could be estimated with

$$D = \frac{\pi}{8640} \left(\frac{d_p k_{id}}{q_e} \right)^2 \quad (11)$$

The external mass transfer could determined from

$$\frac{dq}{dt} = k_{mt} A (C - C_s) \quad (12)$$

where q_t is the amount of metal ions adsorbed at time t (mmol.g^{-1}), k_{id} is the intraparticle diffusion rate constant (mmol.g^{-1}.time$^{-1/2}$), d_p is the mean particle diameter (m), A is the specific surface area of the sorbent (m^2.g^{-1}), D (m^2.s) is the intraparticle diffusion coefficient, C is the liquid phase bulk concentration at certain moment (mol.L^{-1}), C_s is the concentration in the inner pore sorbent (mol.L^{-1}) and k_{mt} is the liquid-solid mass transfer coefficient (mg.m^{-2}.s^{-1}).

Plots of q_t versus $t^{1/2}$ [eq. (10)] are shown in Figure 8. Initial curved with steep sloped portions are attributed to the bulk diffusion or exterior sorption rate which is very high. Only the subsequent linear portions can be attributed to intraparticle diffusion; plateau portions represent the equilibrium.

The earlier behavior is encountered when sorption to the porous sorbents considered as, mesopores may act as micropores because of the potentially formation of water layers on the pore walls.[43] The total specific surface area was measured by BET method (S_{BET}) and corrected using t- plotting diagrams (S_t); 733.64 m^2.g^{-1} and 731.25 m^2.g^{-1} were recorded. By fractionation of porous texture, PAAc-AN-TV surface was viewed as, $\sim$ 70% of the total porosity is macroporous in nature ($\sim$ 50 μm) with hydrophilic character, and the remain part is $\sim$ 35 μm with hard inorganic skeleton. Also, both pore and surface diffusions may play role during the sorption processes to the macroporous structures.[44]

As can be seen in Figure 8, non-linear distribution of the plots and deviation of the curves from the origin, intraparticle diffusion cannot be accepted as the only rate determining step for the sorption of the specified ions on PAAc-AN-TV. On comparison of the k_{id} values calculated from the linear portions of the plots (Table I), it is possible to suggest that intraparticle diffusion, which may play an important role as a rate determining step, is said to be more effective for ^{134}Cs than $^{152+154}$Eu ions. This fact originates as, the k_{id} value for ^{134}Cs (1.4122 mmol.g^{-1}.h$^{-1/2}$) is less than that for $^{152+154}$Eu (1.57737 mmol.g^{-1}.h$^{-1/2}$). This can be attributed to the relatively small radius of the hydrated ^{134}Cs and $^{152+154}$Eu ions.

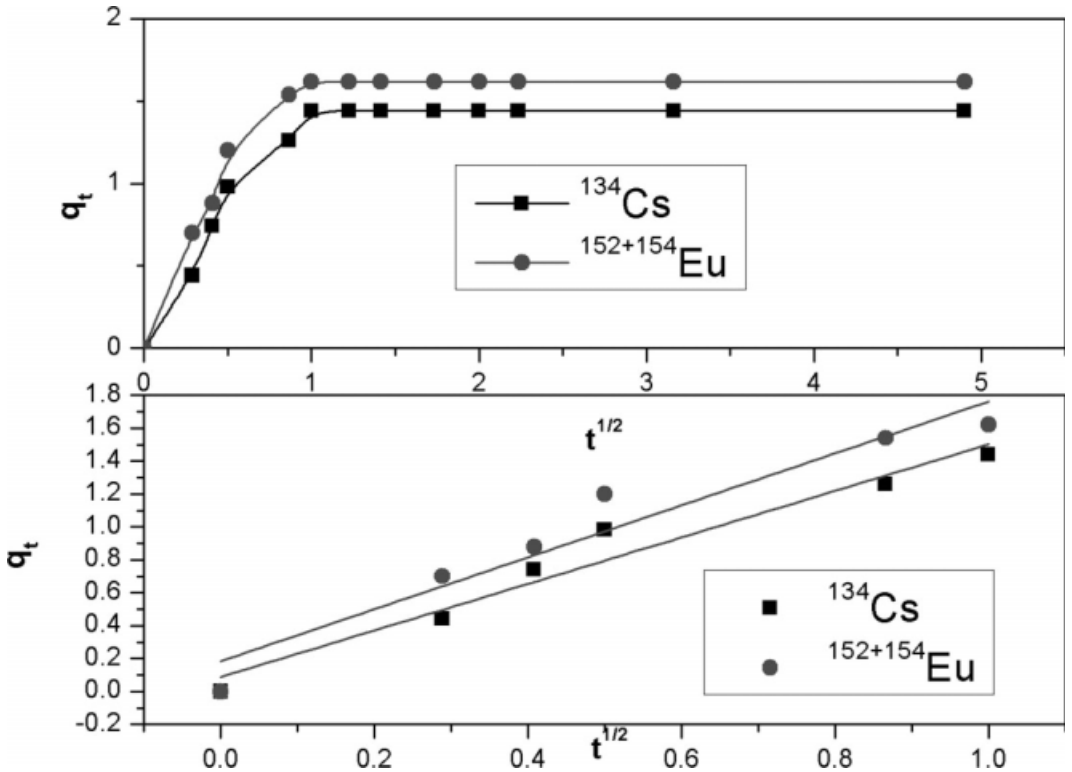

Figure 8 Influence of square root t on q_t of ^{134}Cs and $^{152+154}$Eu sorbed onto PAAc-AN-TV.

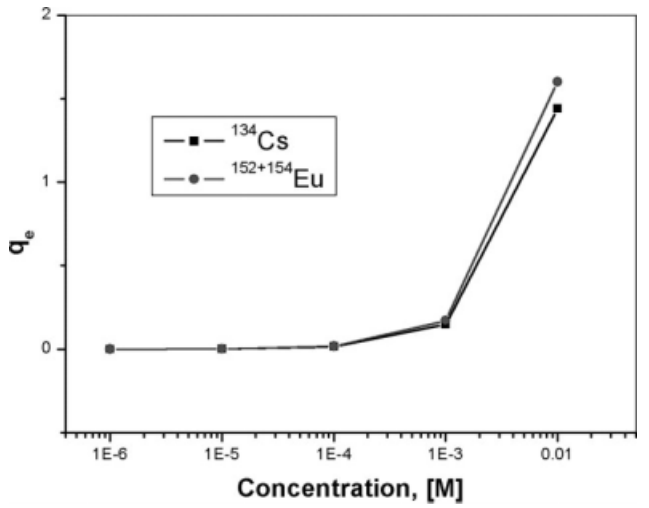

Figure 9 Effect of concentration on q_e of ^{134}Cs and $^{152+154}$Eu sorbed onto PAAc-AN-TV.

Sorption capacity

The effect initial concentrations of ^{134}Cs and $^{152+154}$Eu metal ions on the equilibrium sorption capacities are shown in Figure 9. The sorption capacities were increased with increasing the initial concentrations and reached a maximum after 0.01*M* which represents the maximum sorption capacity of the composite which may be theoretically predicted after that point. This behavior could be explained with the high driving force for the mass transfer, which is similar to that obtained in sorption of divalent cations on dithiocarbamated-sporopollenin.[1] Since, the analysis of the sorption isotherms is important for design purposes, experimental data were analyzed with sorption isotherm models of known equilibrium parameters, namely, Langmuir, Freundlich and D–R models.

Langmuir isotherms

Modeling the monolayer coverage of the sorption surfaces is proposed by Langmuir and assumes that sorption occurs on a structurally homogeneous adsorbent and all the sorption sites are energetically identical, i.e., the sorption of a molecule or an ion on a given site is independent of its neighboring site occupancy. Since adsorption is limited to monolayer coverage, the linearised form of the Langmuir equation[45] is given as:

$$\frac{1}{q_e} = \frac{1}{Q^o} + \frac{1}{bQ^oC_e} \tag{13}$$

where q_e is the amount of solute adsorbed on the surface of the adsorbent (mmol.g^{-1}), C_e is the equilibrium ion concentration in solution (mmol.L^{-1}), Q^o is the maximum surface density at monolayer coverage and b is the Langmuir sorption constant (L.mmol^{-1}). The plots of $1/q_e$ versus $1/C_e$ may give straight lines and the Langmuir constants can be calculated.

Freundlich isotherms

To model the multilayer sorption, Freundlich equation is derived that postulates the heterogeneity of surfaces; its linearised form[46] is given by the following equation:

$$\log q_e = \log K_F + \frac{1}{n}\log C_e \tag{14}$$

where q_e is the equilibrium solute concentration in the adsorbent phase (mmol.g^{-1}), C_e the equilibrium concentration of the solute (mmol.L^{-1}), K_F the Freundlich constant (mmol.g^{-1}) which indicates the sorption capacity and represents the strength of the adsorptive bond and n is the heterogeneity factor. The plots of logq_e versus logC_e may give straight lines and K_F and n values can be calculated from the intercept and slope of these lines.

The constants calculated from Langmuir and Freundlich equations based on Figures 10, 11 are given in Table II. On comparison of the R^2 values, we can conclude that sorption isotherm data obtained for the metal ions studied on PAAc-AN-TV can be described by either and/or Langmuir equation. The correlation coefficients for sorption of the specified ions are nearly the same. This is an apparent contradiction between the two models, which may be later explained by the nature of the adsorbent surface and porosity. In some cases, surface modification can be introduced from one phase to the other.[1,47] The Langmuir constant Q^o indicates the sorption capacity of the sorbent. As it can be seen from Table II, Q^o values were found to be 0.458 and

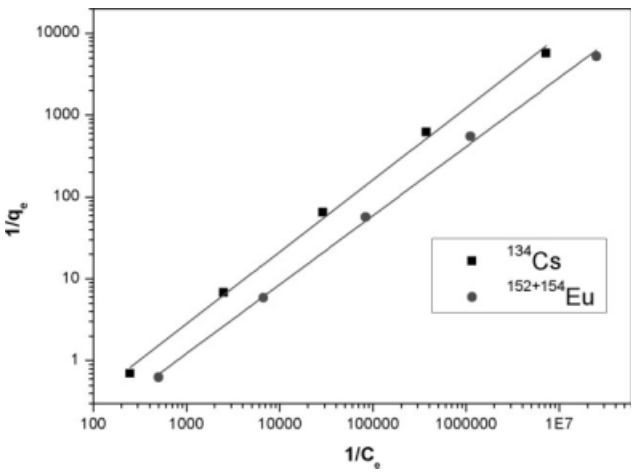

Figure 10 Langmuir isotherms of ^{134}Cs and $^{152+154}$Eu sorbed onto PAAc-AN-TV.

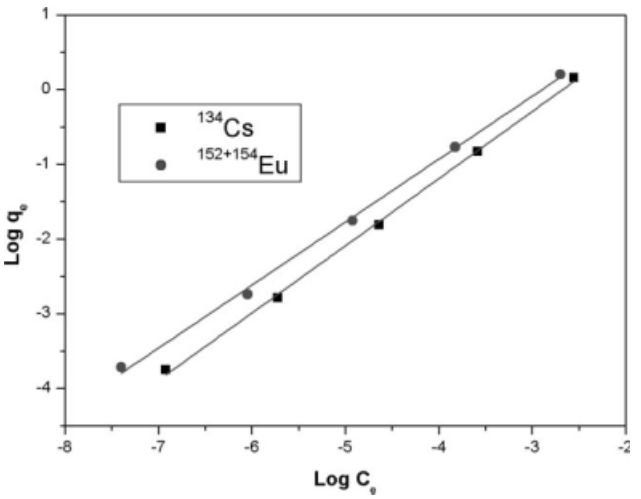

Figure 11 Freundlich isotherms of ^{134}Cs and $^{152+154}$Eu sorbed onto PAAc-AN-TV.

0.41 mmol.g^{-1} for ^{134}Cs and $^{152+154}$Eu, respectively. These sorption capacities are higher than the sorption capacities obtained on sorption of Cu^{2+}, Pb^{2+} and Cd^{2+} on some chelating resins given as 0.2734, 0.4572, and 0.0631 mmol.g^{-1}, respectively.[1] Also, these capacities are higher than the monolayer coverage of some uranyl ionic species and tetravalent thorium ionic entities on some unsaturated polyester styrene formulations given as 0.204 and 0.166 mmol.g^{-1}.[48] As can be seen from Table II, these sorption capacities obtained from Freundlich model are of greater values than Langmuir constants and also higher than that obtained in case of the aforementioned divalent, and also tetravalent and hexavalent cations[1,48] This can be explained by the strength of the bonds between the sorbate and PAAc-AN-TV.

D–R isotherms

In D–R model, sorption on single type uniform pores is adopted. In this manner, the D–R isotherm is an analogue of Langmuir type in a more general postulation that it does not assume a homogeneous surface or constant sorption potential.[49] The D–R isotherm is given as:

$$Q = Q_m \exp(-k\varepsilon^2) \tag{15}$$

and the linearised form of the equation is given by:

$$\ln Q = \ln Q_m - k\varepsilon^2 \tag{16}$$

where ε (Polanyi Potential) is [$RT \ln(1+(1/C_e))$], Q is the amount of solute adsorbed per unit weight of adsorbent (mmol.g^{-1}), k is a constant related to the sorption energy (mmol^2.kJ^{-2}), Q_m is the sorption capacity (mmol.g^{-1}).

The values of Q_m and k were calculated from the intercept and slope of the D-R plots and presented in Table II. The mean free energy of sorption (E) can be calculated from the corresponding k values using the equation:

$$E = \frac{1}{\sqrt{-2k}} \tag{17}$$

Since, Langmuir and Freundlich isotherms do not provide precise sorption mechanisms, the magnitude of E based on Figure 12 in D-R model is considered as a useful mean for estimating the type of sorption process. If this value is between 8 and 16 kJ.mol^{-1}, sorption process can be explained by ion exchange.[44] In this study, for ^{134}Cs and $^{152+154}$Eu ions E values lies in this range; 8.731 and 9.316 kJ.mol^{-1} are estimated, respectively. The E values obtained are found to be comparable to those obtained in case of adsorption of U(IV) and Th(IV) on different unsaturated polyester styrene formulations (8.3-13.9 kJ.mol^{-1})[48]. Therefore, it is possible to conclude that sorption mechanism of ^{134}Cs and $^{152+154}$Eu on PAAc-AN-TV can be explained with an ion exchange process.

Sorption thermodynamics

The sorption dependencies on temperature of ^{134}Cs and $^{152+154}$Eu on PAAc-AN-TV are given as plots of the equilibrium constant values, (K_c) as a function of temperature (Fig. 13). The K_c values increased with increase in temperature and showed the endothermic nature of the sorption. Thermodynamic parameters, namely, free energy change (ΔG^o), enthalpy change (ΔH^o), and entropy change (ΔS^o) can be estimated using the following equations.

$$\Delta G^o = -RT \ln K_c \tag{18}$$

$$\Delta G^o = \Delta H^o - T\Delta S^o \tag{19}$$

TABLE II
Langmuir, Freundlich and D-R Isotherm Constants

	Langmuir parameters			Freundlich parameters			D-R parameters			
Metal ion	Q^o (mmol.g^{-1})	b (L.mmol^{-1})	R^2	K_F (mmol.g^{-1})	n	R^2	Q_m (mmol.g^{-1})	k (mol^2.kJ^{-2})	E (kJ.mol^{-1})	R^2
Cs^+	4.58E-01	2.48E+00	0.99638	254.8376	1.112087	0.99842	2.798406	0.006558	8.731914	0.96162
Eu^{3+}	4.10E-01	2.90E+00	0.99762	275.9559	1.186324	0.99762	3.027418	0.00576	9.31695	0.95842

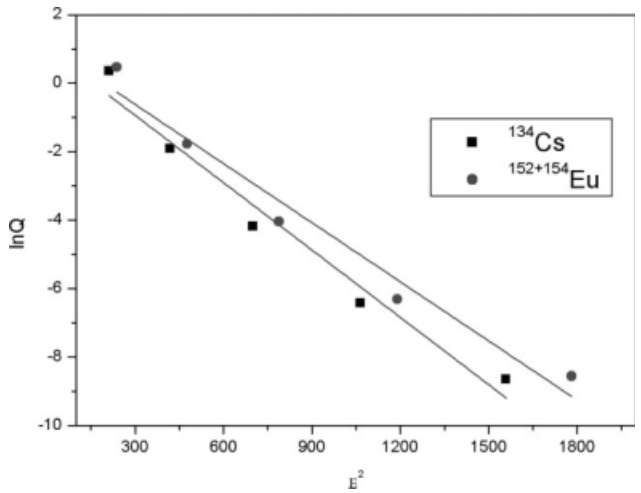

Figure 12 D-R isotherms of ^{134}Cs and $^{152+154}$Eu sorbed onto PAAc-AN-TV.

$$\log K_c = \frac{\Delta S^o}{2.303R} - \frac{\Delta H^o}{2.303RT} \quad (20)$$

where R is gas constant (kJ.mol^{-1}.K^{-1}) and T is the absolute temperature in Kelvin. Table III summarizes the thermodynamic parameters as could be calculated from the slope and intercept in Figure 13. Positive ΔH° values represents the endothermic nature of the sorption process; values between 20.9 and 418.4 kJ mol^{-1}, are heats of chemical reactions.[48] ΔH° values were found as 46.92 and 5.4 kJ.mol^{-1} for ^{134}Cs and $^{152+154}$Eu, respectively, as comparable values for the chemical sorption processes. According to the calculated E values previously described, the adsorption mechanism of ^{134}Cs and $^{152+154}$Eu onto the sorbent could be viewed as an ion exchange process. These results are also in good agreement with the calculated E values and support the possibility

TABLE III
Thermodynamic Parameters for Sorption of ^{134}Cs and $^{152+154}$Eu Onto PAAc-AN-TV

Metal ion	ΔH^o (kJ.mol^{-1})	ΔS^o (J.mol^{-1}.K^{-1})	T (K)	ΔG^o (kJ.mol^{-1})	R^2
Cs^+	46.92749	164.7081	298	−2.15553	0.87235
			303	−2.97907	
			313	−4.62615	
			323	−6.27323	
			333	−7.92031	
Eu^{3+}	50.40036	180.3952	298	−3.3574	0.83319
			303	−4.25938	
			313	−6.06333	
			323	−7.86728	
			333	−9.67123	

of the chemisorption that is the rate determining step in the sorption process. Negative values of ΔG° (−2.15 to −7.92 kJ.mol^{-1} in case of Cs^+ and −3.35 to −9.67 kJ.mol^{-1} in case of Eu^{3+}adsorption at different temperatures) indicate the spontaneous nature of the reactions[1,].[48] ΔS° contributions to the sorption process values were found to be positive due to the exchange of the metal ions with more mobile ions present on the exchanger. In this study, a case of physisorption, which may also contribute to the total sorption process, is encountered, in which, water molecules released from the hydrated metal ions or from the sorption surface may also cause an increase in the entropy.

Mechanism and surface modeling

In this study, different models were used to model the surface of PAAc-AN-TV. To emphasize on the surface adsorbate-adsorbent interactions, effect of some competing ions should be studied. Figure 14 shows the distribution coefficient of ^{134}Cs and $^{152+154}$Eu in presence of corresponding monovalent

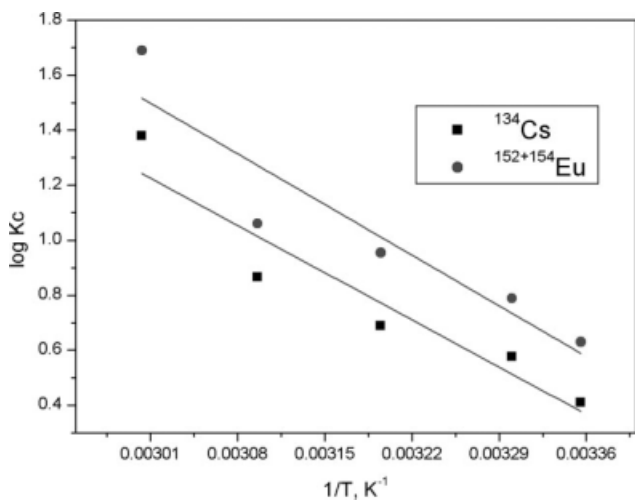

Figure 13 Equilibrium constant-temperature dependence of ^{134}Cs and $^{152+154}$Eu sorbed onto PAAc-AN-TV.

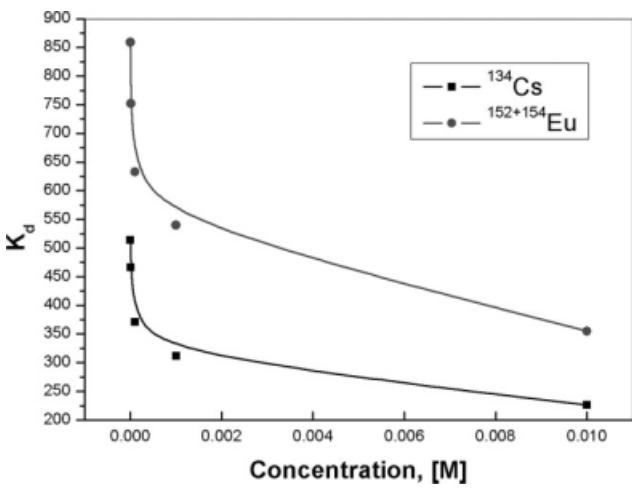

Figure 14 Effect of NaCl and $FeCl_3$ concentration on K_d of ^{134}Cs and $^{152+154}$Eu sorbed onto PAAc-AN-TV.

and trivalent ions, namely, Na^+ and Fe^{3+}, respectively. As shown in the Figure, the K_d markedly decreases with increasing the salt content in solution. This character may be explained according to the following scenarios:

The first is based on that the surface of the adsorbent can viewed as a Double Shell Model (DSM) spheres inside which the inorganic part of the composite is resident; outside the core, a larger shell of the organic part, PAAc-AN, is present. The outer part has a macroporous structure, while the inner part is mesoporous.

The outer part of the DSM is characterized by hydrophilic behavior and therefore highly adsorbed of ^{134}Cs and $^{152+154}Eu$ species in a high rate as indicated by the high Freundlich capacity values. These values are directly related to the strength of the bond as indicated by high values of enthalpy change. However, the n values are greater than unity that reflects the surface heterogeneity in its real state.

The inner part of the DSM has a hard skeleton inside which, the movement of ions is slow and is considered the rate determining barrier in the sorption process.

The porosity inside the surface of the composite DSM is apparent and may be changed according the type of the interacting species. Macroporous surfaces with hydrophilic nature may act as mesopores, while mesoporous textures may act as micropores. This can be interpreted by considering either the hydration shells around ^{134}Cs and $^{152+154}Eu$ ions, or the type of the species.

The entropy change of the system is of positive values for all studied ions. This can be understood by determination of the different ionic species in solution at different pHs and various concentrations. As seen in Figure 14, the amounts of ^{134}Cs and $^{152+154}Eu$ adsorbed by the composite decrease with increase in monovalent sodium and trivalent ferric ions in solution. This can be explained by the competition of other species with cesium and europium ions especially at different pH values.

In case of $^{152+154}Eu$ and trivalent iron at pH less than 4, H^+, $FeCl^{2+}$, Eu^{3+}, Fe^{3+}, $EuCl^{2+}$, $FeOH^{2+}$, $FeCl_2^+$, $Fe(OH)_2^+$, and $EuNO_3^{2+}$ are present. Between pH 4 and 8, Eu^{3+}, Fe^{3+}, $EuNO_3^{2+}$, $EuCl^{2+}$, $EuOH^{2+}$, $FeCl_2^+$, $Eu(OH)_2^+$ are found. Beyond pH 8, only hydrolyzed europium and iron species as $Eu(OH)_4^-$, $Fe(OH)_2$, cubic $Eu(OH)_3$ precipitate, may be present beside orthorhombic Fe_2O_3 crystals.[50]

However, in competition between Na^+ and ^{134}Cs, adsorption, free Cs^+, H^+, Na^+ ions, and $NaNO_3$ are present from pH 2 to pH 10.4, beyond which sodium hydroxide may appear.

To complete our model, the DSM, the outer shell of the composite may stretched, which can be mapped as a semi-flat area of different positions that represents different active sites that have different energies. These sites may interact with the aforementioned species according to either size of the transferred species from the bulk to the active site or to wall potential of the site itself. These large probabilities led to greater values of positive entropies; 164.7 and 180.39 $J.mol^{-1}.K^{-1}$ are registered in case of Cs^+ and Eu^{3+} adsorption, respectively.

CONCLUSIONS

PAAc-AN-TV novel composite was prepared and characterized with different tools. The composite would have greater radiation chemical and thermal stabilities than the conventional composites, and over the base polymeric materials used in its preparation, namely, PAAc and PAN. Also, the sorption capacity of PAAc-AN-TV was larger than the usual composites used in treatment of radioactive nuclides, especially when high bond strengths between the binding ions and the active sites were obtained. More over, the reactor design including, its dimensions could enhanced.

Sorption of ^{134}Cs and $^{152+154}Eu$ on PAAc-AN-TV was fitted with different approaches. Kinetic and equilibrium fitting methods were used to determine the rate determining step and the type of adsorption predominant. The obtained results were correlated to the structure of the composite with emphasize on the proposed DSM. The proposed model succeeded in explanation of the kinetic and thermodynamic parameters especially, the contradictions encountered between Langmuir and Freundlich approaches. Therefore, the DSM could be stated as:

The DSM can be only applied to composite adsorbents that are mainly composed of inorganic-organic entities. The surface of the adsorbent is viewed as a double shell with two distinct sides; the core is the inorganic component, while the outer shell is the organic matrix. The organic shell must be hydrophilic which may be characterized with macro-or meso-porosity, while the inorganic is of mesoporous or microporous nature. The surface of the DS is considered to be heterogeneous, i.e., heterogeneous distribution of the active sites is postulated. The ions move from the bulk of the solution to the DS through mass transfer. The distance taken off by the ions through the outer shell is twice that travelled into the inner shell. The concentration gradient is inversely proportional to the square root of the distance; the diffusion of ions is mainly affected by the hydrophilic nature of the organic part.

However, the DSM should be extended to cover the other composite materials rather than the PAAc-AN-TV composite after postulating its characteristic

mathematical equations. The theoretical approach of the DSM is now under final construction.

References

1. Uenlue, N.; Ersoz, M. Sep Purif Technol 2007, 52, 461.
2. Rengaraj, S.; Kim, Y.; Joo, C. K.; Yi, J. J Colloid Interf Sci 2004, 273, 14.
3. Taty-Costodes, V. C.; Fauduet, H.; Porte, C.; Delacroix, A. J Hazard Mater B 2003, 105, 121.
4. Bailey, E. S.; Olin, T. J.; Bricka, R. M.; Adrian, D. D. Water Res 1999, 33, 2469.
5. Pearson, R. G. J Am Chem Soc 1963, 85, 3533.
6. Kantipuly, G.; Katragadda, S.; Chow, A.; Gesser, H. D. Talanta 1990, 37, 491.
7. Ima, S.; Muroi, M.; Hamaguchi, A. Anal Chim Acta 1980, 113, 139.
8. Murthy, R. S. S.; Ryan, D. E. Anal Chim Acta 1982, 140, 139.
9. Ni, Y. H.; Ge, X. W.; Liu, H.; Zhang, Z. C.; Ye, Q.; Wang, F. Chem Lett 2001, 5, 458.
10. Ni, Y. H.; Ge, X. W.; Zhang, Z. C. Mater Lett 2002, 55, 171.
11. Ni, Y. H.; Ge, X. W.; Zhu, Z.; Zhang, Z. C. J Chem Phys (China) 2002, 15, 393.
12. Ni, Y. H.; Ge, X. W.; Liu, H.; Zhang, Z. C.; Ye, Q. Chem Lett 2001, 9, 924.
13. Ni, Y. H.; Ge, X. W.; Zhang, Z. C. Mater Sci Eng B 2005, 119, 51.
14. Ni, Y. H.; Ge, X. W.; Liu, H. R.; Zhang, Z. C.; Ye, Q. Radiat Phys Chem 2001, 61, 61.
15. Qiao, Z.; Xie, Y.; Li, G.; Zhu, Y.; Qian, Y. J Mater Sci 2000, 35, 285.
16. Brunauer, S.; Emmett, P. H.; Teller, E. J Am Chem Soc 1938, 60, 309.
17. Gregg, S. J.; Sing, K. S. W.Adsorption, Surface Area and Porosity, 2nd ed.; Academic Press: London, 1982.
18. de Boer, J. H.; Lippens, B. C.; Linsen, B. G.; Broekhollf, J. C. P.; van der Heuvel, A.; Osinga, T. H. J. J Colloid Interface Sci 1966, 21, 405.
19. Nakamoto, K. Infrared and Raman Spectra of Inorganic and Coordination Compounds, 6th ed.; John Wiley and Sons: New Jersey, 2009.
20. Mata-Zamora, M. E.; Arriola, H.; Nava, N.; Saniger, J. M. J Magn Magn Mater 1996, 161.
21. Chenga, B.; Leia, M.; Yua, J.; Zhaob, X. Mater Lett 2004, 58, 1565.
22. Vivekanandhan, S.; Venkateswarlu1, M.; Satyanarayana, N. Mater Lett 2004, 58, 2717.
23. Xu, X.; Yin, Y.; Ge, X.; Wu, H.; Zhang, Z. Mater Lett 1998, 37, 354.
24. Chen, D. H.; Chen, Y. Y. J Colloid Interface Sci 2001, 235, 9.
25. Honga, R. Y.; Pana, T. T.; Hana, Y. P.; Lib, H. Z.; Ding, J.; Han, S. J Magn Magn Mater 2007, 310, 37.
26. Nataraj, S. K.; Kim, B. H.; Cruz, M.; Ferraris, J.; Aminabhavi, T. M.; Yang, K. S. Mater Lett 2009, 63, 218.
27. Ni, Y.; Gea, X.; Zhang., Z.. Mater Sci Eng B 2006, 130, 61.
28. Pan, W.; Yang, S. L.; Li, G.; Jiang, J. M. Eur Polym J 2005, 41, 2127.
29. Stamatin, I.; Morozana, A.; Scott, K.; Dumitru, A.; Vulpe, S.; Nastase, F. J Membr Sci 2006, 277, 1.
30. Coşkun, R.; Soykan, C. J Polym Res 2006, 13, 1.
31. Woehlecke, H.; Lerche, D.; Ehwald, R. Proceedings of the X International BRG Workshop on Bio-encapsulation. Cell Physiology and Interactions of Biomaterials and Matrices; Prague, Czech Republic, 26–28 April, 2002; 183.
32. Lagergren, S.; Svenska, B. K. Vaternskapsakad Handlingar 1898, 24, 1.
33. Hanif, M. A.; Nadeem, R.; Bhatti, H. N.; Ahmad, N. R.; Ansari, T. M. J Hazard Mater 2007, 139, 345.
34. Preetha, B.; Viruthagiri, T. Sep Purif Technol 2007, 57, 126.
35. Vijayaraghavan, K.; Palanivelu, K.; Velan, M. Bioresour Technol 2006, 97, 1411.
36. Javed, M. A.; Bhatti, H. N.; Hanif, M. A.; Nadeem, R. Sep Sci Technol 2007, 42, 3641.
37. Pino, G. H.; Mesquita, L. M. S.; Torem, M. L.; Pinto, G. A. S. Miner Eng 2006, 19, 380.
38. Dahiya, S.; Tripathi, R. M.; Hegde, A. G. J Hazard Mater 2008, 150, 376.
39. Vilar, V. J. P.; Botelho, C. M. S.; Boaventura, R. A. R. J Hazard Mater 2007, 149, 643.
40. Ho, Y. Water Res 2006, 40, 119.
41. Ho, Y. S.; McKay, G. Process Biochem 1999, 34, 451.
42. Weber, W. J. Jr.; Morris, J. C. Removal of Biologically-Resistant Pollutants from Waste Waters by Sorption. Advances in Water Pollution Research, Pergamon Press: New York, 1962; 231.
43. Fan, M.; Boonfueng, T.; Xu, Y.; Axe, L.; Tyson, T. A. J Colloid Interf Sci 2004, 281, 39.
44. Kilislioglu, A.; Bilgin, B. Appl Radiat Isot 2003, 58, 155.
45. Langmuir, I. J Am Chem Soc 1918, 40, 1361.
46. Freundlich, H. M. F. Z Phys Chem 1906, 57, 385.
47. Uenlue, N.; Ersoez, M. J Hazard Mater 2006, 136, 272.
48. El-Gammal, B.; Ibrahim, G. M.; El-Nahas, H. H. J Appl Polym Sci 2006, 100, 4098.
49. Rieman, W.; Walton, H. Ion Exchange in Analytical Chemistry, Pergamon Press: Oxford, 1970; 38.
50. Martell, A. E.; Smith, R. M., Eds. NIST Standard Reference Database 46 Version 7.0, NIST: Gaithersburg, USA, 2003.